Science Advances
AAAS

advances.sciencemag.org/cgi/content/full/6/10/eaay4958/DC1

Supplementary Materials for

One-dimensional hexagonal boron nitride conducting channel

Hyo Ju Park, Janghwan Cha, Min Choi, Jung Hwa Kim, Roland Yingjie Tay, Edwin Hang Tong Teo, Noejung Park, Suklyun Hong*, Zonghoon Lee*

*Corresponding author. Email: zhlee@unist.ac.kr (Z.L.); hong@sejong.ac.kr (S.H.)

Published 6 March 2020, *Sci. Adv.* **6**, eaay4958 (2020)
DOI: 10.1126/sciadv.aay4958

The PDF file includes:

Other Supplementary Material for this manuscript includes the following:

(available at advances.sciencemag.org/cgi/content/full/6/10/eaay4958/DC1)

Movie S1 (.mp4 format). Transformation of 558-N to 6′6′-N configuration.
Movie S2 (.mp4 format). Formation of atomically sharp twin boundary at EK edge.

Section S1. The stacking structures of hBN

Due to its bi-elemental composition, hexagonal boron nitride (hBN) can assemble in various stacking structures, with two different types of interlayer orientations. In this study, we use the symbols [BN] and [NB] (a hexagonal structure rotated by 60° relative to [BN]) to represent hexagonal structures defined by the order of atoms clockwise from the apex (fig. S1A).

There are six possible stacking structures with high symmetry, depending on the rotation (0° or 60°) and translation of the hexagons relative to the bottom layer, termed "A" (fig. S1B). The structure in which all atoms in the upper and lower layers are in the same positions and the same orientations is termed "AA stacking". The structures in which the upper layer is translated to the center of a hexagon in the lower layer are called either "AB stacking" or "AC stacking". Both AB and AC stacking are also known as "Bernal stacking," which is easily found in graphite. The AB and AC stackings are distinguished in this paper since the consequential atomic configurations at stacking boundaries are different even though AB and AC have the same level of structural stability. The configuration in which the N atoms are on top of the B atoms is defined as the "AB stacking structure," and the opposite is true for "AC stacking" in this paper. The prime (′) mark indicates that the orientation of the upper layer is rotated by 60° relative to the lower layer like [BN]/[NB] or [NB]/[BN].

The stability of a stacking structure depends strongly on the interactions between the atoms in the upper layer with those in the lower layer. Since differing atoms (B-N) experience an attractive force, while identical atoms (B-B or N-N) have a repulsive interaction, AA′ is the most stable structure, and AB and AC are less stable (13, 14).

Section S2. Identification of the stacking structure and the number of layers of hBN using DF-TEM

The stacking structure and the number of layers of hBN can be determined by measuring the intensity of dark-field transmission electron microscopy (DF-TEM) images. The intensity of the DF-TEM image depends on the interference of electron waves produced though the specific lattice periodicity, corresponding to the diffraction spot being used in acquiring the DF-TEM image. Thus, it is sensitive to the lateral translation between layers. As shown in fig. S1C, for AA′ stacking, which has no lateral translation, the intensities of the first- (Φ1) and second-(Φ2) order families of diffraction spots increase with the number of layers since the electron wave diffracted from one layer always interferes constructively with the wave diffracted from the other layers. In contrast, for Bernal stacking, like AB or AC, in which one layer of the lattice is translated with a lattice spacing of 3a/2 relative to another, a phase difference is caused depending on the diffraction spot. The electron wave interferes destructively along the 2.16 Å (Φ1) lattice periodicity but it still interferes constructively along the 1.25 Å (Φ2) lattice periodicity (16). For ABC stacking, the Ø1 diffraction spots show completely destructive interference since the phases of the electron wave scattered from the AB and AC stackings are opposites (37).

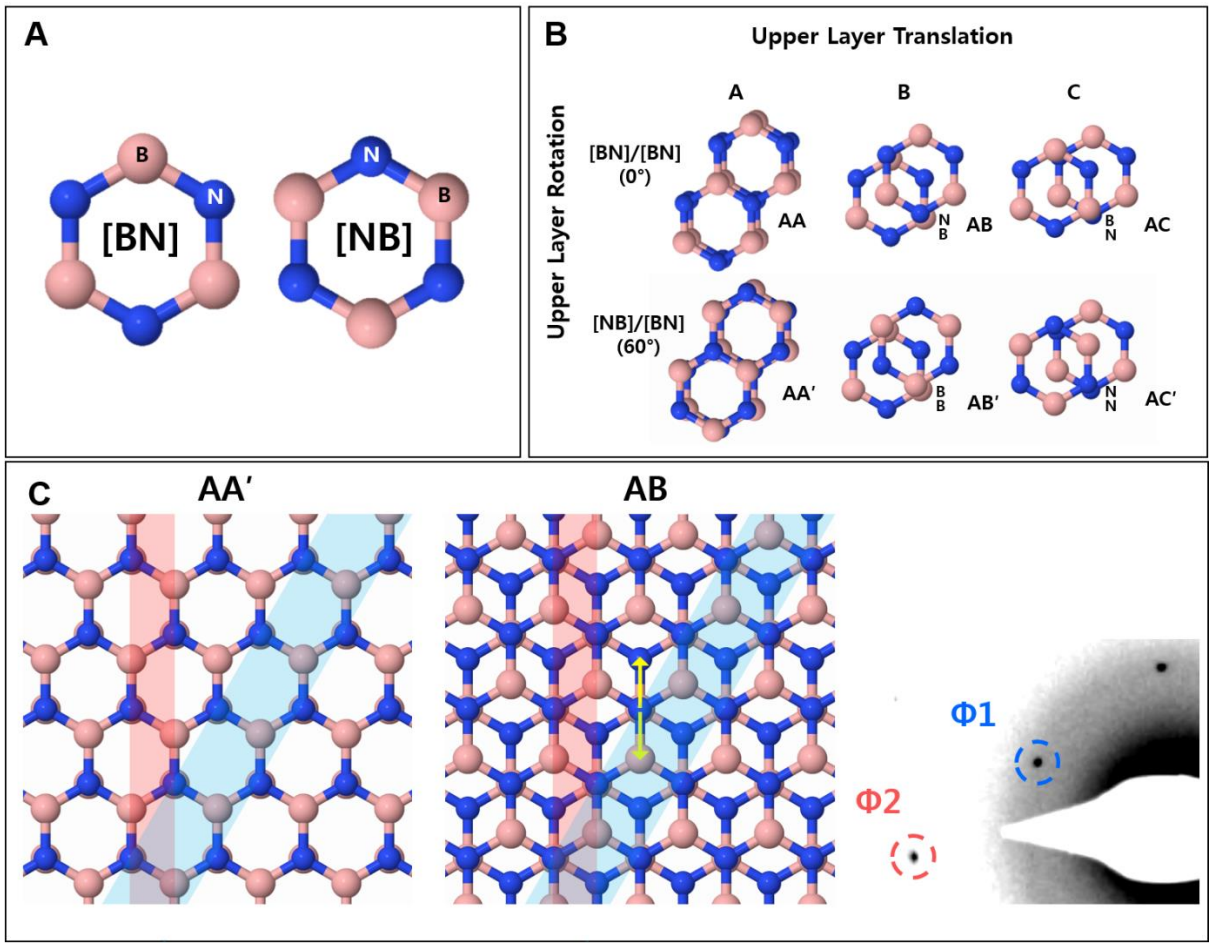

Fig. S1. Stacking structures of hBN. (**A**) Atomic models of the [BN] and [NB] configurations. Boron and nitrogen atoms are represented in pink and blue, respectively. (**B**) High-symmetry stacking structures of hBN. (**C**) The lattice periodicity of 2.16 Å (1. 25 Å) is highlighted in blue (red) and corresponds to the diffraction spot Ø1 (Ø2) in the SAED patterns. Displacement vectors for the AB or AC structures are marked in yellow.

Section S3. A transition region at AA′/AB stacking boundary

As discussed in the previous section, bright contrast in a DF-TEM image means constructive interference of the waves diffracted from a given lattice. Especially for the second-order diffraction spots (Φ2), the DF-TEM images always have brighter contrast with increasing numbers of layers if the hBN layers are oriented in a high-symmetry stacking structure (see the six structures in fig. S1B). Thus, the dark line displayed in Fig. 2C, is the locus of positions of atoms in one layer that are shifted relative to other layers, causing destructive interference (16, 25-27). Considering that an SAED pattern shows one set of hexagonal spots (fig. S2D), the relative positions of the atoms shift gradually, without any rotation of the dark-line region. That is, the dark line indicates the presence of a transition region at the boundary between the two different stacking structures. The higher mag TEM images of Fig. 2E and 2F directly demonstrate this. The red dashed lines are the outlines of triangular defects caused by prolonged electron-beam irradiation. The opposite directions of the red outlines, which are divided by the black dashed line, indicate a change of phase between [BN] and [NB]; the orientations of triangular defects are in opposite directions in [BN] and [NB] structures since the electron beam always creates N-terminated triangular defects. The atomic-scale image for the region marked with a black arrow in fig. S2F loses the original hexagonal lattice contrast, which indicates a transition region, not in high-symmetry stacking, between different stacking structures. The various stacking structures noted in Fig. 2B are identified by using the characteristics of DF-TEM images that the image contrast from Φ1a and Φ1b are alternatively bright for odd (even) numbers of layers when they have the AB (AC) stacking structure (38).

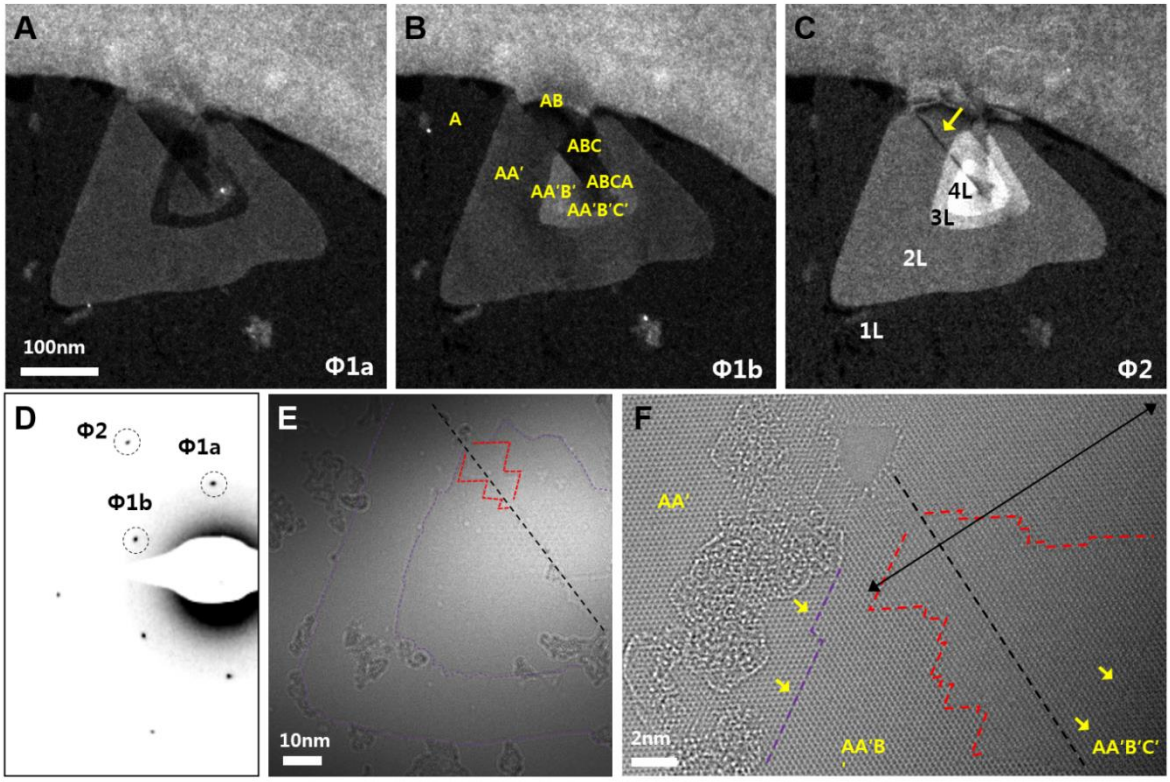

Fig. S2. Transition region at AA′/AB stacking boundary. (**A** to **C**) DF-TEM images from the diffraction spots Φ1a, Φ1b, and Φ2, respectively, in (**D**). The different stacking structures are designated in (B), and the numbers of layers are given in (C). (**E** and **F**) The corresponding TEM images under low (E) and high (F) magnification after electron-beam irradiation. The red dashed lines show the triangular defects caused by the TEM electron beam. The region indicated by the black dashed lines in (E) and (F) matches the region represented by the dark line in (C).

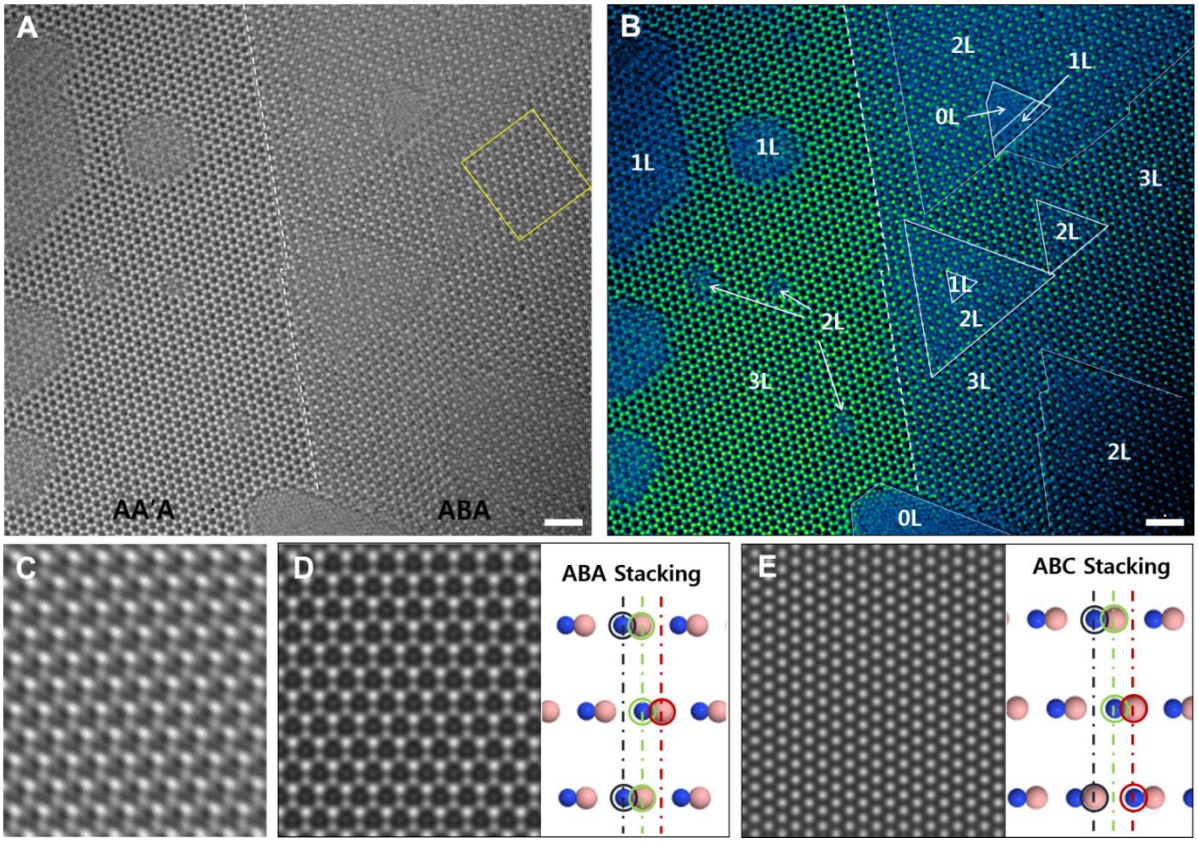

Fig. S3. AA′A- and ABA-stacked trilayer hBN. (**A**) HR-TEM image at the same region in Fig. 2A after tens of seconds of electron-beam irradiation. (**B**) False-colored image of (A) for better visualization of the etched layers. Colors change from green to blue as the number of layers decreases from 3 L to 0 L (vacuum) in each of the AA′- and AB-stacked regions. Both the AA′- and AB-stacked regions are tri-layers. Scale bars, 1 nm. (**C**) Magnified TEM image of yellow boxed region in (A). (**D** and **E**) Simulated TEM images and atomic models of cross-section of hBN with ABA stacking (D) and ABC stacking (E). Boron and nitrogen atoms are represented by pink and blue, respectively.

The ABA stacking shows stronger contrast in positions where three atoms are superimposed, weaker contrast for two atoms, and faint for one atom at the given position. In the meantime, there is no contrast difference in ABC stacking because two atoms are piled up at all positions. The HR-TEM image matches the ABA stacking configuration.

Section S4. Deduction of atomic configuration of AA′A/ABA stacking boundary

Depending on the orientation of [BN] or [NB] and the stacking order of AB or AC, the AA′A/ABA stacking boundary in zigzag direction can have four different types of twin boundaries (fig. S4). They are denoted by (1) 6′6′-N, (2) 44-B, (3) 6′6′-B, and (4) 44-N, where 6′6′ (44) represents an oblong hexagonal (rhombal) ring and -N(-B) denotes the N(B) mirror plane at the twin boundary. The 6′6′-N (44-B) twin boundary is formed at the center of an A′/B (A′/C) layer when the first layer A has [BN] orientation. The 6′6′-B (44-N) twin boundary is formed at the center of the A′/C (A′/B) layer when the first layer A has the [NB] orientation.

We performed two verification steps to determine which of the four possible structures best fit our observations shown in Fig. 2A. First, the orientation of the N-terminated triangular defect highlighted in yellow in Fig. 2A matches that of either (1) 6′6′-N or (2) 44-B (see fig. S3 for a clear image of a triangular defect produced by an electron beam). In addition, the intensity profile across the twin boundary (fig. S5) proves that the 6′6′-N structure matches the experimental result shown in Fig. 2.

We only considered four twin boundaries along zigzag direction since our triangular hBN islands are terminated with zigzag edges. Refer to the study by O. Cretu et al. (39) for atomic configuration at a boundary along armchair direction, which reported 4|8 (square-octagon) defects in monolayer hBN.

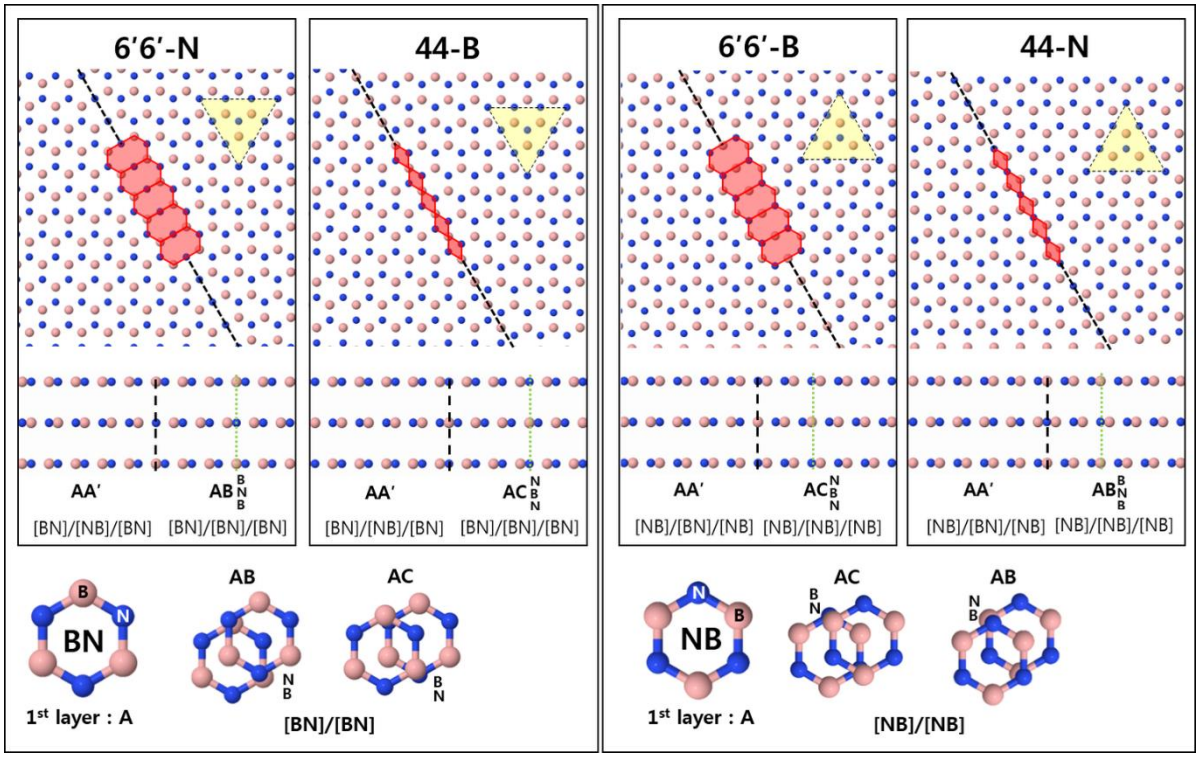

Fig. S4. Atomic structures of the four possible stacking boundaries. Each top-view image is from the middle layer of the stacking structure represented below it. A 6′6′-N (44-B) twin boundary is formed at the center of an A′/B (A′/C) layer when the first layer A has the [BN] orientation. A 6′6′-B (44-N) twin boundary is formed at the center of an A′/C (A′/B) layer when the first layer A has the [NB] orientation. Boron and nitrogen atoms are represented by pink and blue, respectively.

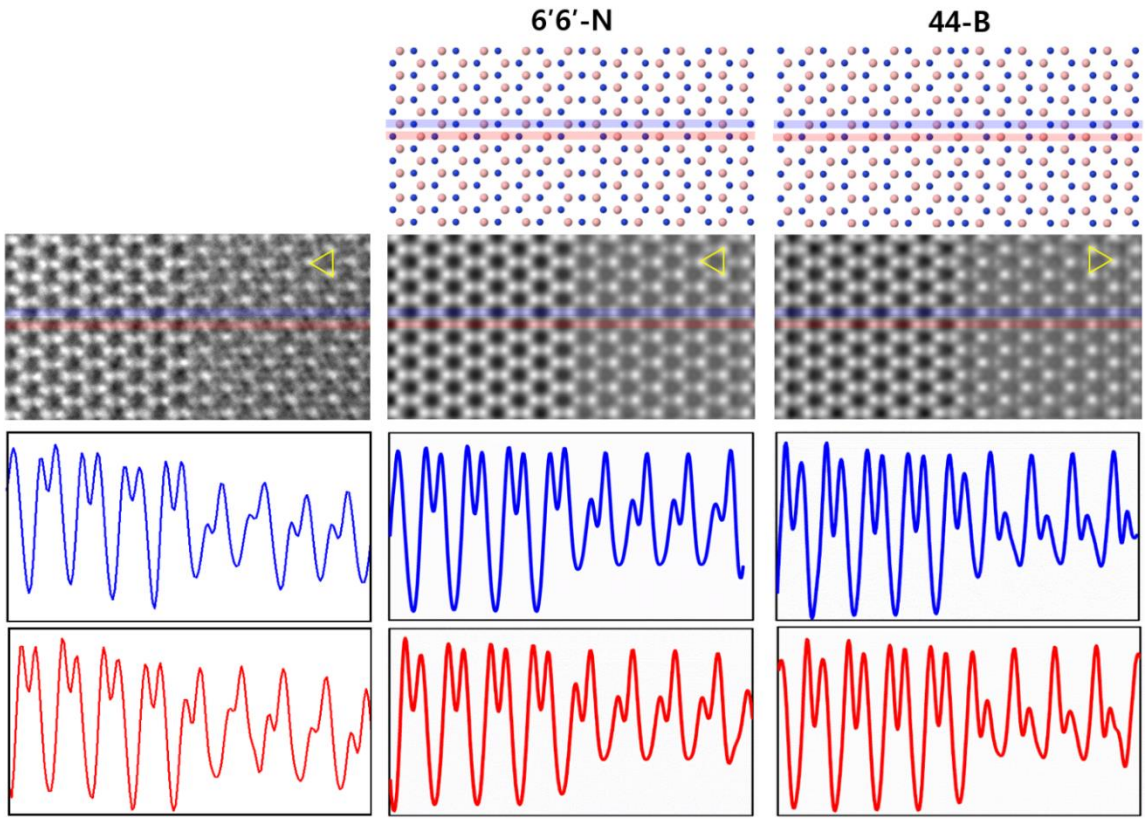

Fig. S5. Intensity profiles across the AA′/AB stacking boundary. Intensity profiles along the blue and red lines in the experimental image (left) and the simulated images of the 6′6′-N and 44-B structures, respectively. Boron and nitrogen atoms are represented by pink and blue, respectively.

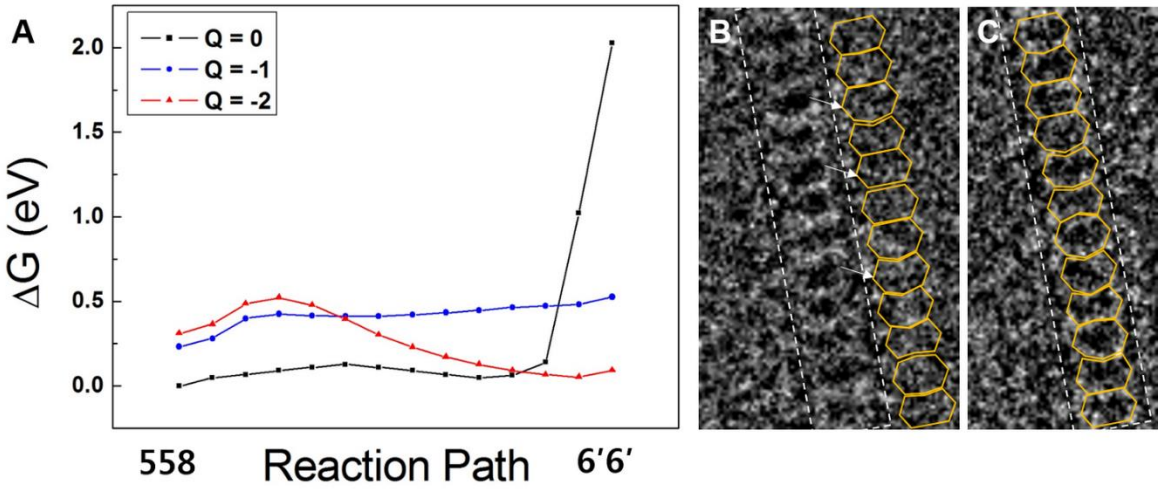

Fig. S6. The energy barrier for 558 configuration changing to 6′6′ configuration and IFFT images showing oscillation of 6′6′ configurations. (**A**) The energy barrier for 558 configuration changing to 6′6′ configuration when the total charges of system are 0, -1 and -2. 558 configuration changes to 6′6′ configuration if it overcome the energy barrier of ~ 0.2 eV with -2 charge state in the hBN nanoribbon structure. (**B** and **C**) IFFT Images showing oscillation of 6′6′ configurations from two different frames at the same twin boundary region. A little change in N-N distance over time but still have dominant 6′6′ and close to 6′6′ configurations along the twin boundary.

Section S5. Stability of exposed and sandwiched 6′6′ twin boundary

Atomically sharp AA′/AB stacking boundaries are commonly found and clearly visible in tri-layer case as shown in fig. S7A. Atomically sharp AA′/AB stacking boundary in bi-layer, where one side of twin boundary should be exposed to ambient condition, are found but the "bare" 6′6′ configuration is not revealed under TEM since the boundary is always covered by hydrocarbon as shown in fig. S7B. This is because such "defect" line imbedded in perfect hBN hexagonal lattice has higher chemical reactivity. This suggests that a twin boundary sandwiched in the middle of a tri-layer, and thus protected by the top and bottom layers is much more stable than that lying in a bi-layer, wherein the twin boundary is exposed to ambient conditions. This does not mean monolayer 6′6′ twin boundary cannot exist alone. According to DFT calculations, the formation energy of hBN sheet embedding atomically sharp twin boundaries (558-N, 558-B) are all stable in mono-, bi-, and tri-layer. And MD simulations for 558 configuration in mono- and tri-layer turned to 6′6′ configuration favorably. In other words, 6′6′ twin boundary itself is theoretically stable to exist alone, if no foreign atom is wandering around as the system of simulations. In the real system, however, the exposed side was always covered by hydrocarbon. Therefore, the 6′6′ twin boundary is only clearly observable in tri-layer or more layer if sandwiched, since the top and bottom layer are protecting the twin boundary from the attachment of hydrocarbon outside onto the surface.

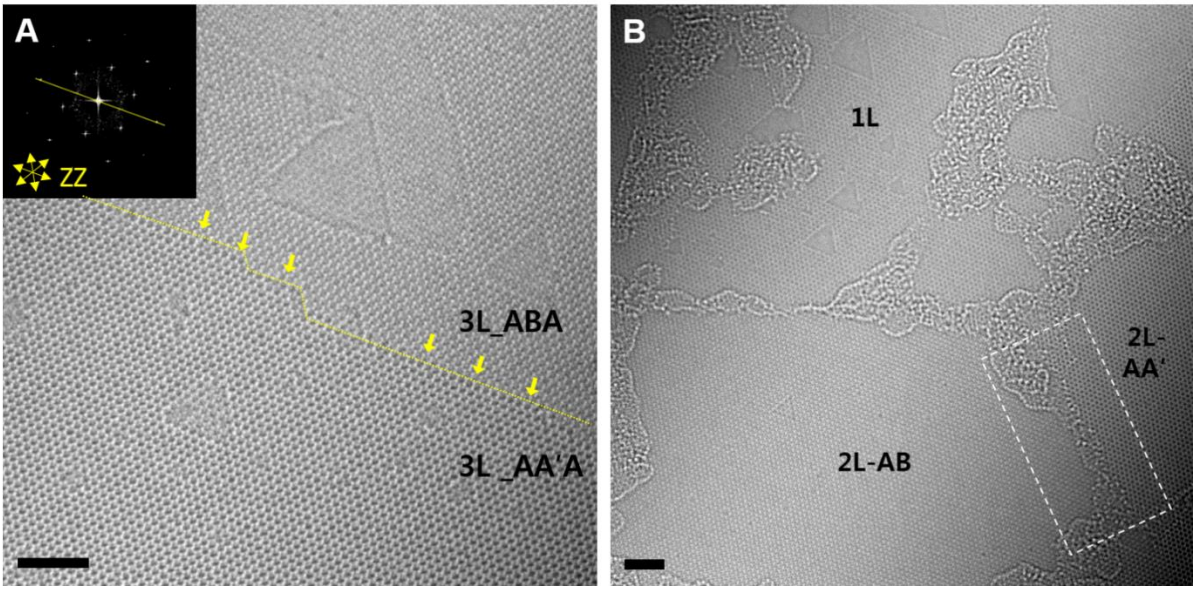

Fig. S7. Atomically sharp stacking boundary at a trilayer and a bilayer hBN. Figure (**A**) shows another example of a tri-layer AA′A/ABA stacking boundary. The stacking boundary is clearly visible. Figure (**B**) shows that AA′- and AB-stacked hBN bi-layers stitch together perfectly without any transition region, although the boundary is covered by adsorbates on the surface (white-boxed area). Scale bars, 2 nm.

This provides an evidence that a twin boundary sandwiched in the middle of a tri-layer, and thus protected by the top and bottom layers is much more stable than that lying in a bilayer, wherein the twin boundary is exposed to ambient conditions.

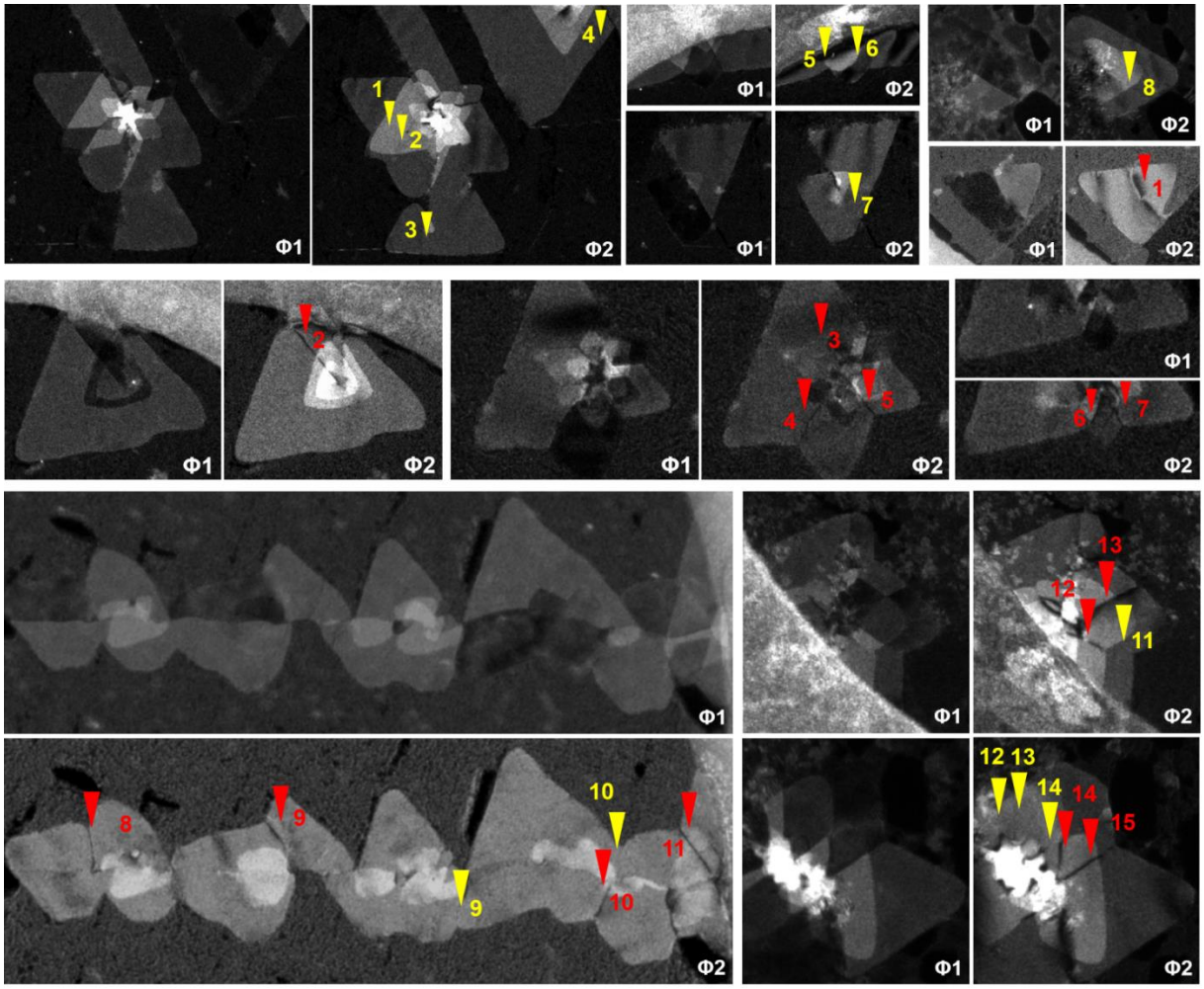

Fig. S8. Probability of finding stacking boundary with an abrupt change or with a transition region. Yellow marked areas indicate atomically sharp stacking boundaries, where show no dark line in DF-TEM images acquired from the second order diffraction spot (Φ2). And red marked areas present stacking boundaries with transition regions with dark lines in Φ2 DF-TEM images. Among 29 regions, 14 atomically sharp stacking boundaries and 15 stacking boundaries with transition regions were observed (almost half-half probability).

Section S6. Identification of [NB]-AC stacking for bilayer hBN from the 1|2-layer boundary

The stacking information whether AB or AC stacking can be identified from the layer boundary of AB-stacked hBN. We cannot figure it out inside the sheet without edge structure since they look exactly the same. (As we mentioned above, AB and AC stacking is distinguished since they cause the different atomic configurations at the stacking boundaries.)

For example, see the 1|2-layer boundary in Fig. 5A with the [NB] orientation, which is inferred from the orientation of the triangular defect whose apex is pointing upward (marked in yellow in the upper part of Fig. 5A). We made AB and AC stacking model of the 1|2-layer boundary in [NB] orientation and compared with the experimental image (fig. S9). Comparing the relative positions of the hexagonal and triangular patterns (orange lines) along bright contrast at the 1|2-layer boundary, the experimental image matches with the AC stacking structure. Thus, it is confirmed that the bilayer region in Fig. 5A has [NB]-AC stacking. In addition, with the contrast difference at the positions where atoms exist or not along the boundary, we can determine the hexagonal edge is ‘closed’ as usual, or ‘open’ also known as the EK edge. See the main text and Fig. 5B for further analysis of the EK edge (40).

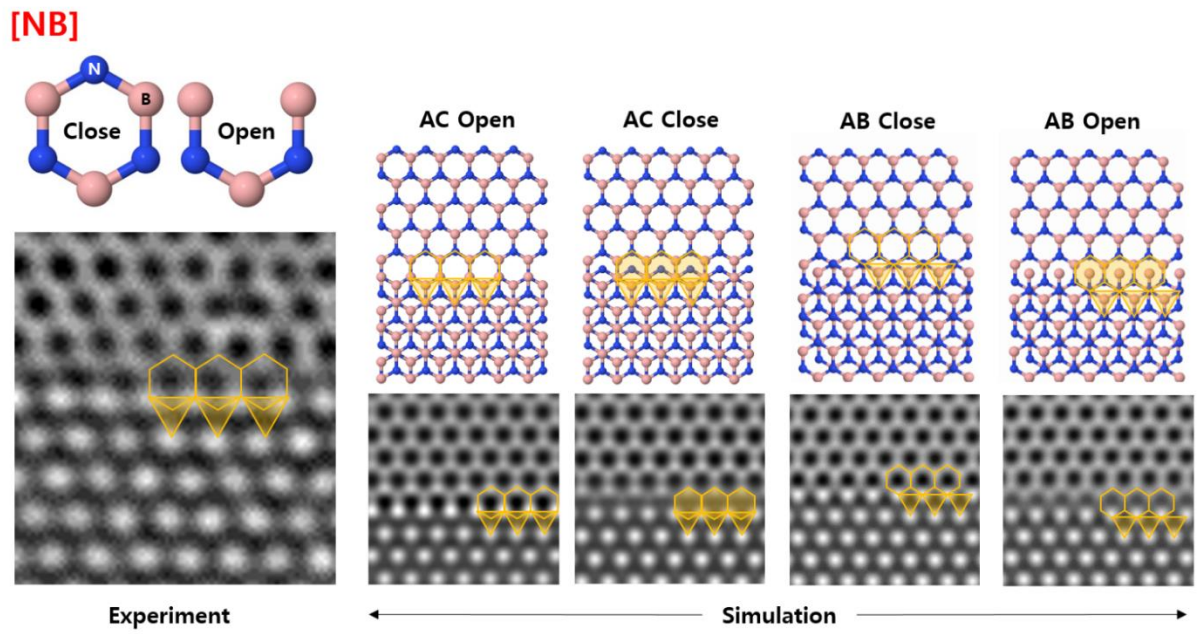

Fig. S9. Comparison of experimental HR-TEM image with simulated images of open- and closed-edge conformations at the 1|2-layer boundary of AB-stacked hBN. The experimental image matches the open EK edge conformation. Boron and nitrogen atoms are represented by pink and blue, respectively.